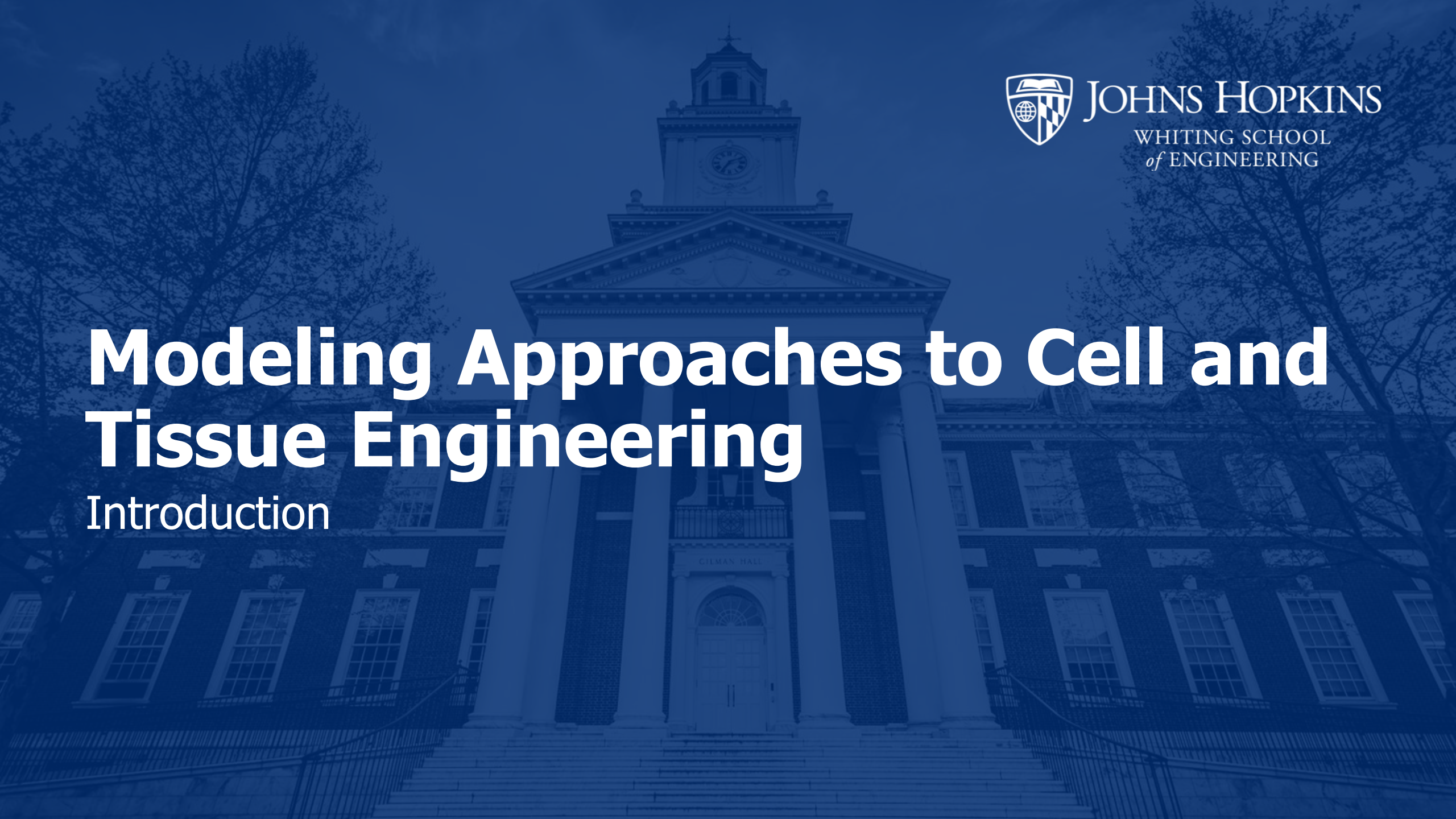

JOHNS HOPKINS
WHITING SCHOOL
of ENGINEERING

Modeling Approaches to Cell and Tissue Engineering

Introduction

Modeling Approaches to Cell and Tissue Engineering 585.743

Alexander A. Spector

Lecture 1

1. Computational Domain of a Multi-Cellular System
2. Cell Transitions in Rule-Based Lattice Method
3. Example of Tumor Growth Simulation. Analysis of Rule-Based Algorithm.
4. Simulation of Angiogenesis within Porous Scaffolds
5. Simulation of Brain Tumor Growth under the Effect of Vasculature
6. Simulation of of Epithelial Cell-Substrate Interaction
7. Simulation of Bone Healing
8. Simulation of Bone Healing. Finite Element Method
9. Simulation of Multi-Stage ASC Myogenesis under the Action of Harmonic Strain
10. Cell Subpopulations during ASC Myogenesis

Sketch of Computational Domain of a Multi-Cellular System

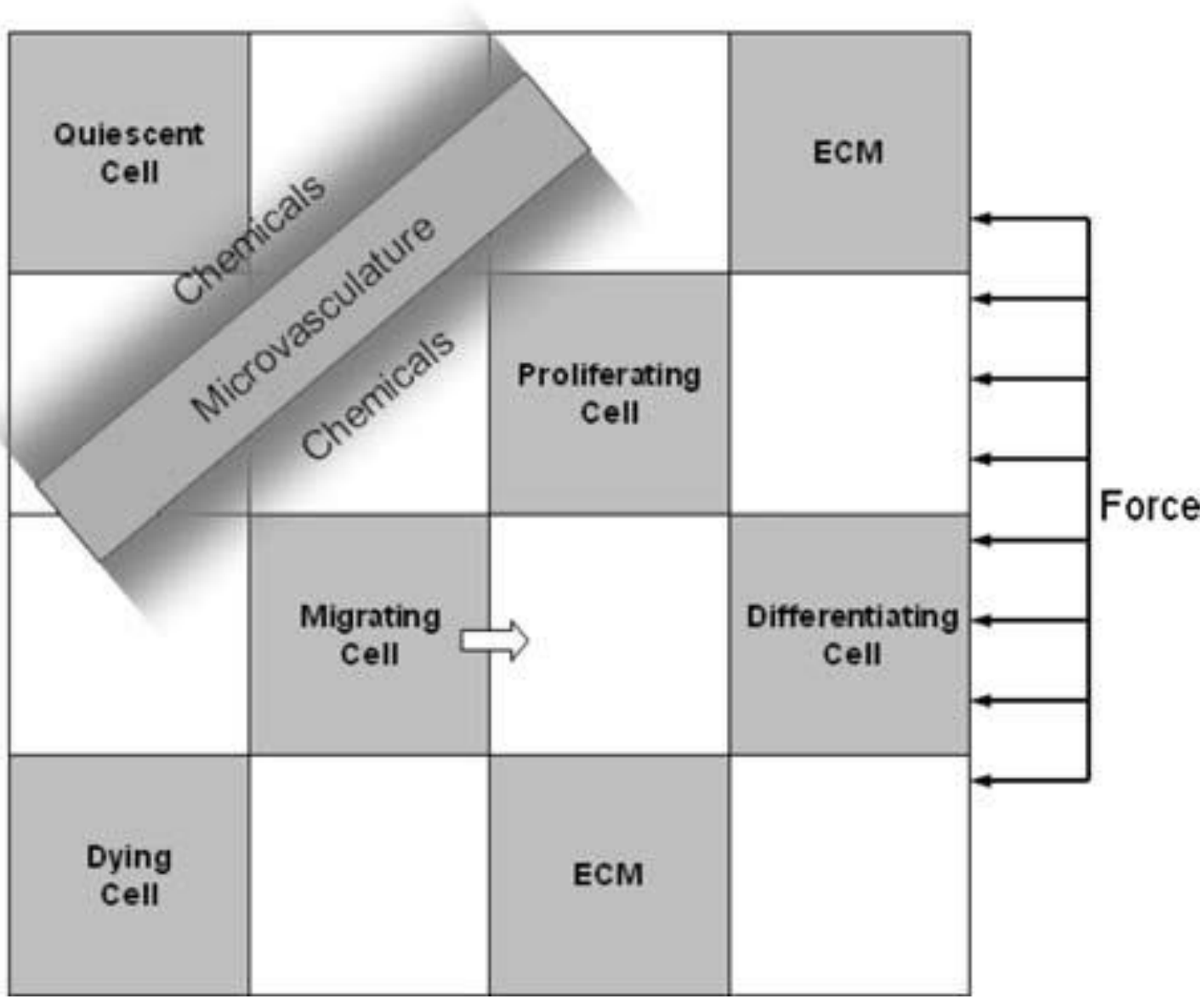

Fig. 1 Schematic of computational domain of rule-based simulation for multi-cellular system. Cell behaviors include proliferation, migration, apoptosis/necrosis, differentiation. The environmental factors include extracellular matrix, chemicals, microvasculature, and forces (From Hwang et al. 2009).

Rule-Based Cell Transitions in a Multi-Cellular System

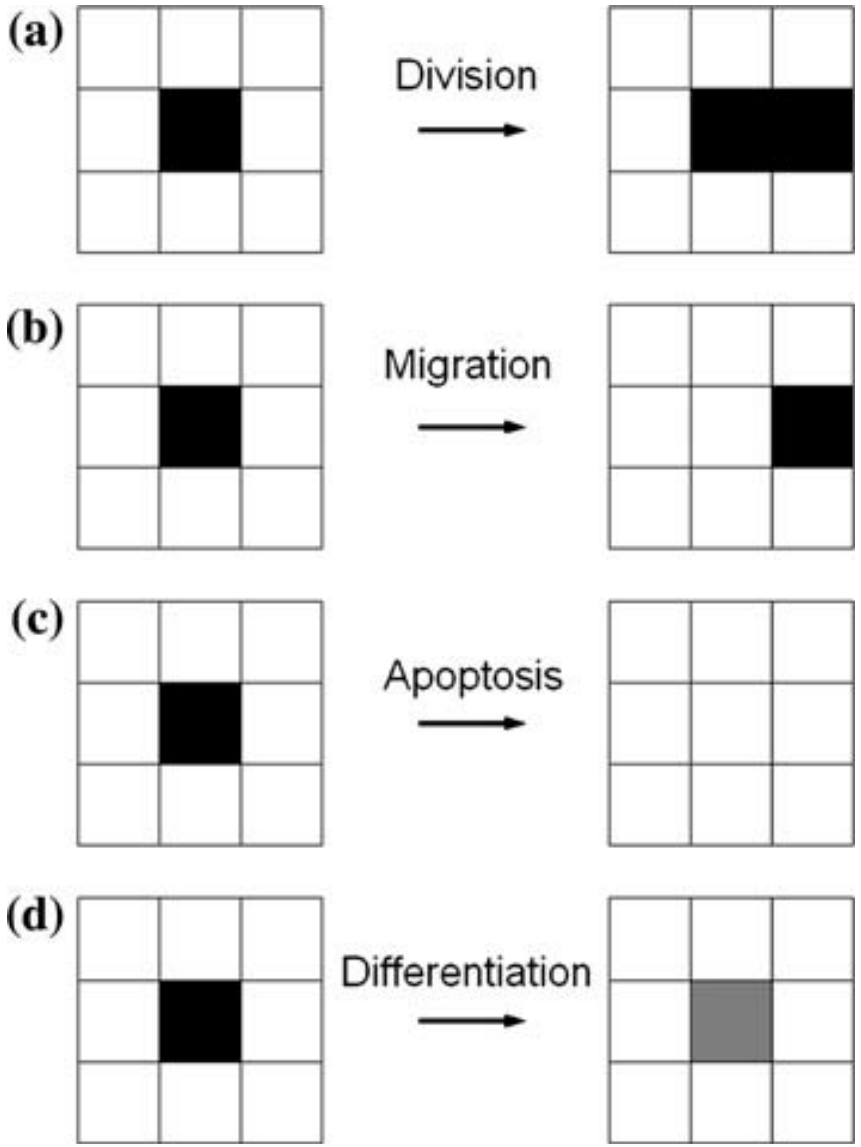

Fig.2 Schematic of cell behavior implementation on the lattice. Black and grey elements represent cells. White elements represent empty spaces. (a) When a cell divides, a new cell is created. (b) When a cell migrates, the location of the cell changes. (c) When a cell dies, the cell disappears from the lattice. (d) When a cell differentiates, the cell becomes a different cell (From Hwang et al. 2009).

Example of Tumor Growth Simulation

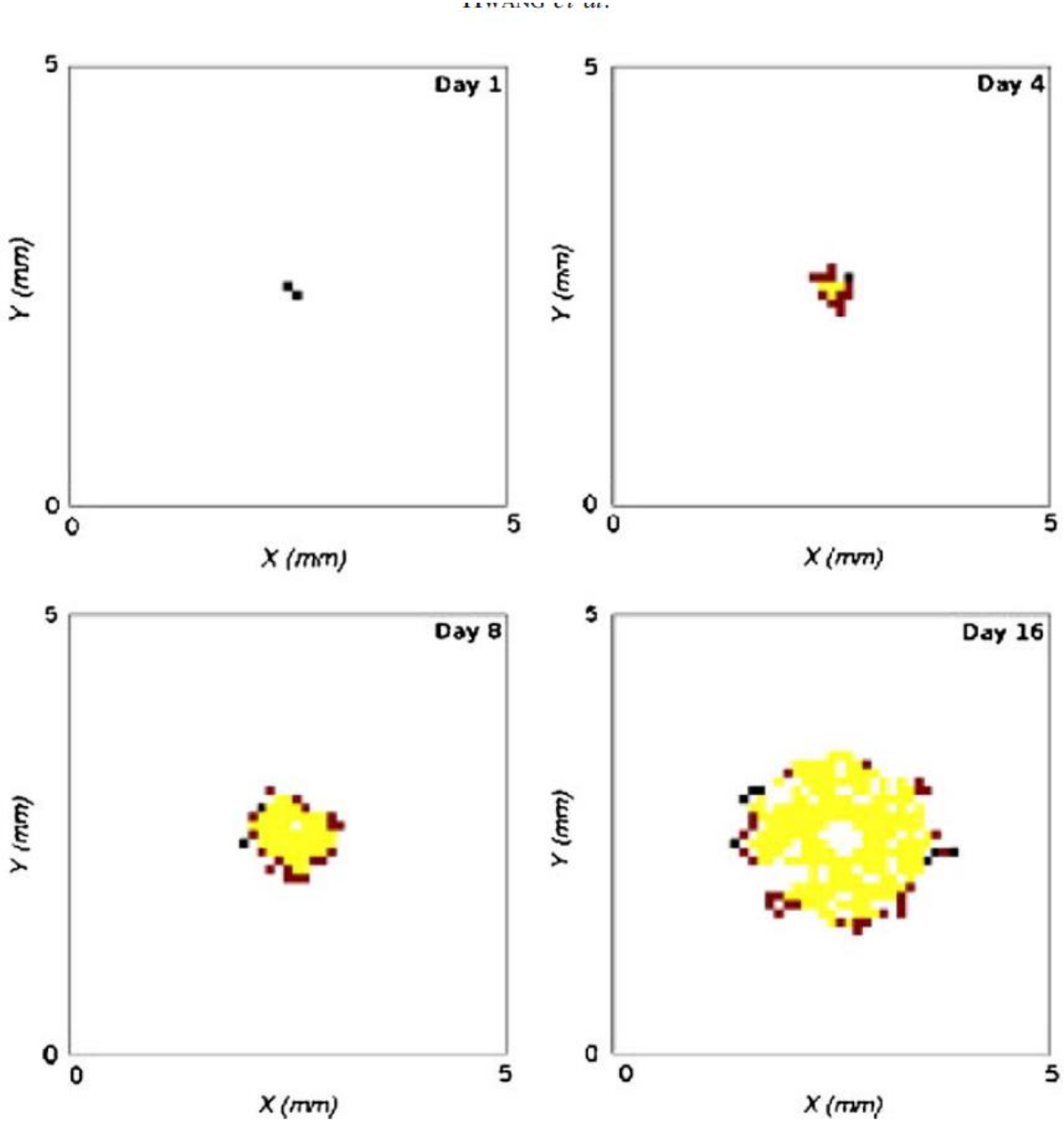

Fig.3 Simulation of in vitro multi-cellular spheroid tumor growth. Each lattice site contains 400 biological cells. Cells in aerobic proliferation (black), anaerobic proliferation (red), aerobic quiescence (orange), and anaerobic quiescence (yellow) are shown. (From Piotrowska and Angus, 2009)

Diagram of Gene-Protein Interaction Network Used in Rule-Based Tumor Growth Simulation (from Zhang et al. 2009)

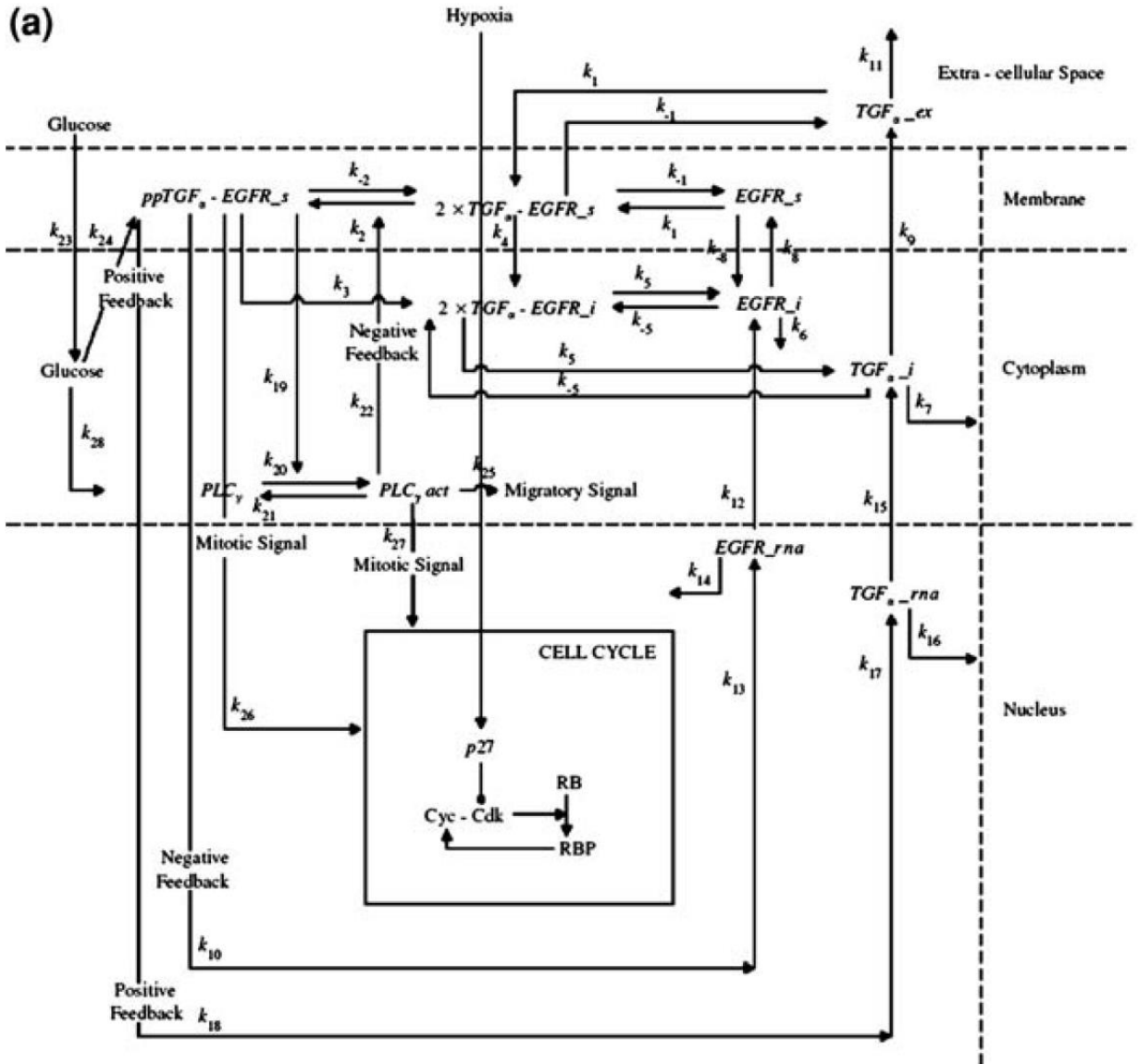

Rules Governing Cell Transitions in Tumor Growth Simulation-1

Next, we initialize approximately 500 agents or cancer cells in the center of the 3D
lattice, each of which is equipped with the type of EGFR gene–protein network detailed in Fig. (a)
At every simulation step, each cell is ‘checked’ or updated according to the following rules:
If the glucose concentration is lower than a set cell death threshold, the cell enters into apoptosis.
If the glucose concentration is between this cell death and a set quiescent threshold, the cell turns quiescent, a reversible state.
If the glucose concentration is higher than this quiescent threshold, the cell utilizes the values of the components of its EGFR gene–protein interaction network to process the ‘phenotypic decision’:

Rules Governing Cell Transitions in Tumor Growth Simulation-2

If the cell is in a proliferative state (a PLC_{γ} concentration change over time is higher than a set proliferation threshold), it runs through its cell cycle at a speed that is correlated with the available oxygen concentration. After completing its cell cycle which, in the model, varies between 22 and 26 h, the cell chooses an empty neighborhood with the highest glucose concentration to replicate and to place its offspring. And, again, if no unoccupied neighboring space can be found, this cell turns quiescent until space becomes available.

At the end of each simulation step, the chemoattractants are replenished by the nutrient source and diffuse across the virtual brain slice volume.

When the first cell (migratory or proliferative) enters the location of the vessel

(75, 75, 75), the simulation is terminated.

Simulation Snapshot of Evolving Tumor System at Three Consecutive Time Moments (migratory cells are in red, proliferative cancer cells are in blue)

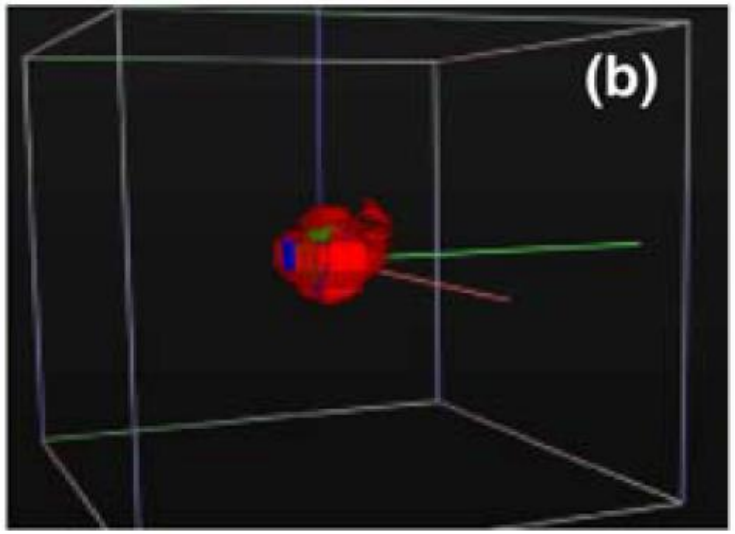

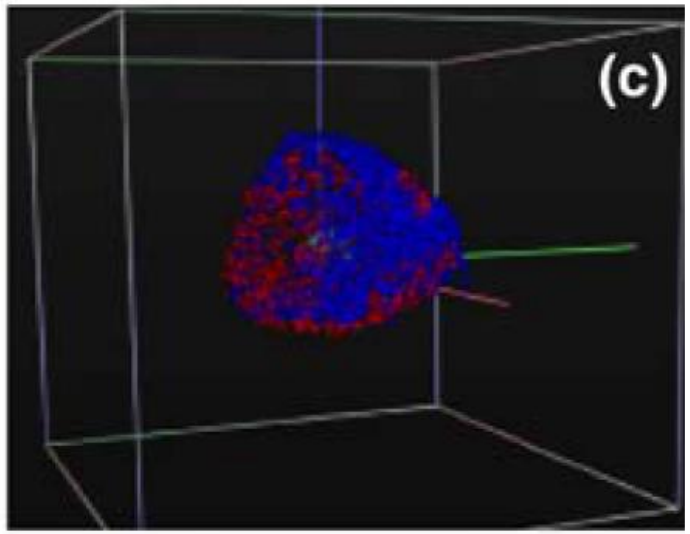

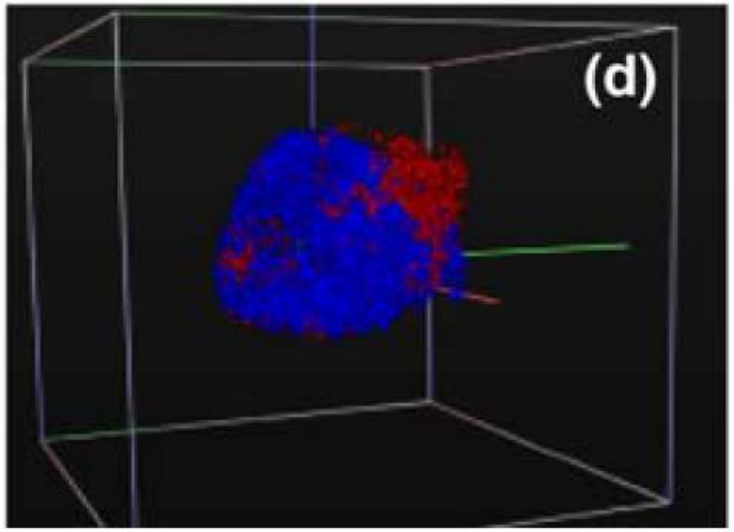

Simulation of Angiogenesis in a Porous Scaffold

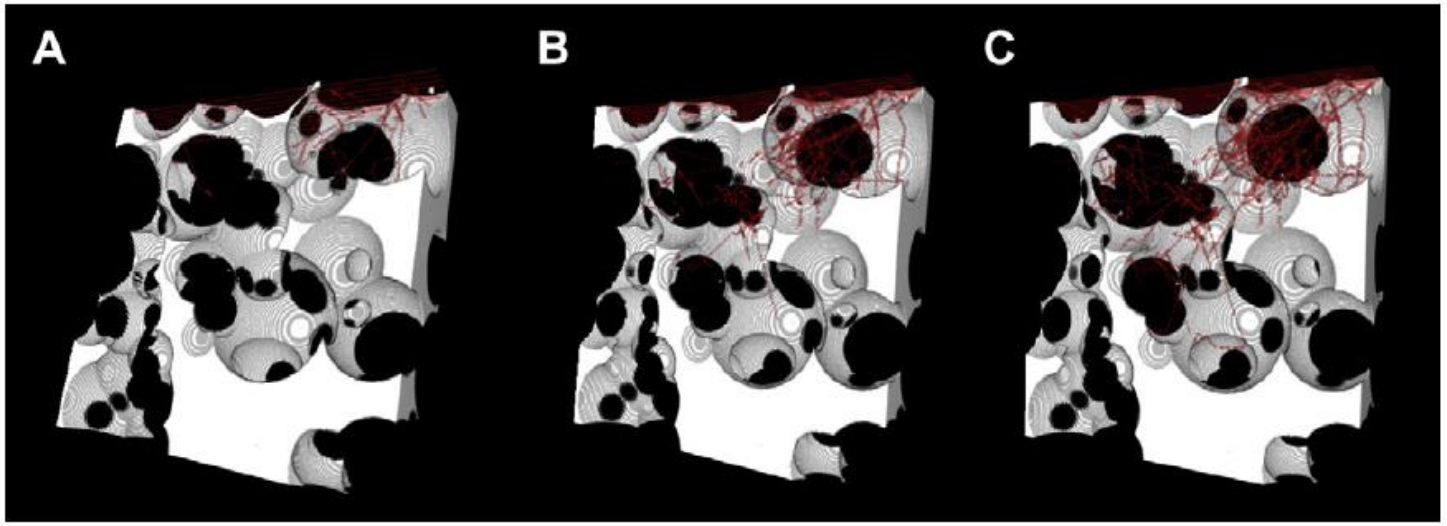

Fig. 9 3D renderings of heterogeneous scaffold vascularization after (A) 1, (B) 3, and (C) 5 weeks from the start of simulation within a scaffold with mean pore size of 400 mm,overall scaffold porosity 80% and pore size distribution is 75 mm. The region of the scaffolds shown is 2000 x 2000x 1000 mm. (From Mehdizadeh et al., 2013)

Fig. 8 A 3D agent-based model was developed to simulate sprouting angiogenesis within model porous polymeric scaffolds. Geometrical scaffold properties such as pore size, interconnectivity of homogeneous scaffolds, size distribution and overall porosity were shown to have a critical impact on vascularization. Larger pore sizes, higher porosities, and increased pore size distributions resulted in a general increase in vascularization. Computational models are useful and valuable for optimization of biomaterial design and development of hypotheses prior to the performance of costly and time-consuming laboratory or animal studies

Example of Tumor Growth Simulation. Effect of Vasculature

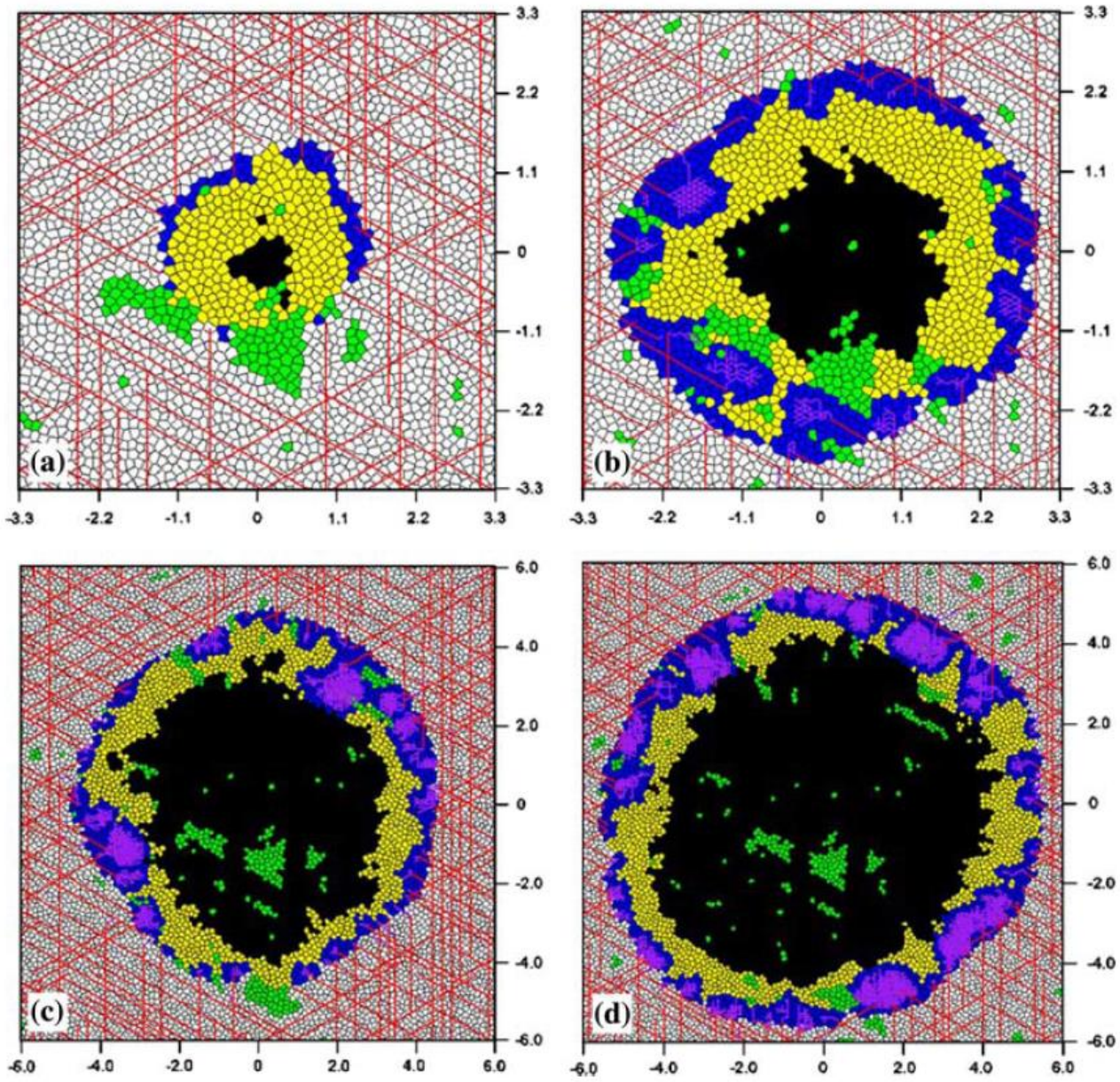

Fig. 4. Simulation of brain tumor growth under the effect of vasculature. Straight lines are microvascular network. (a) Day 40, (b) day 70, (c) day 100, and (d) day 130. Proliferative cells (blue), hypoxic cells (yellow), necrotic cells (black), and apoptotic cells(green) are shown. (From Gevertz and Torquuato, 2006)

Epithelial Cells-Substrate interacton

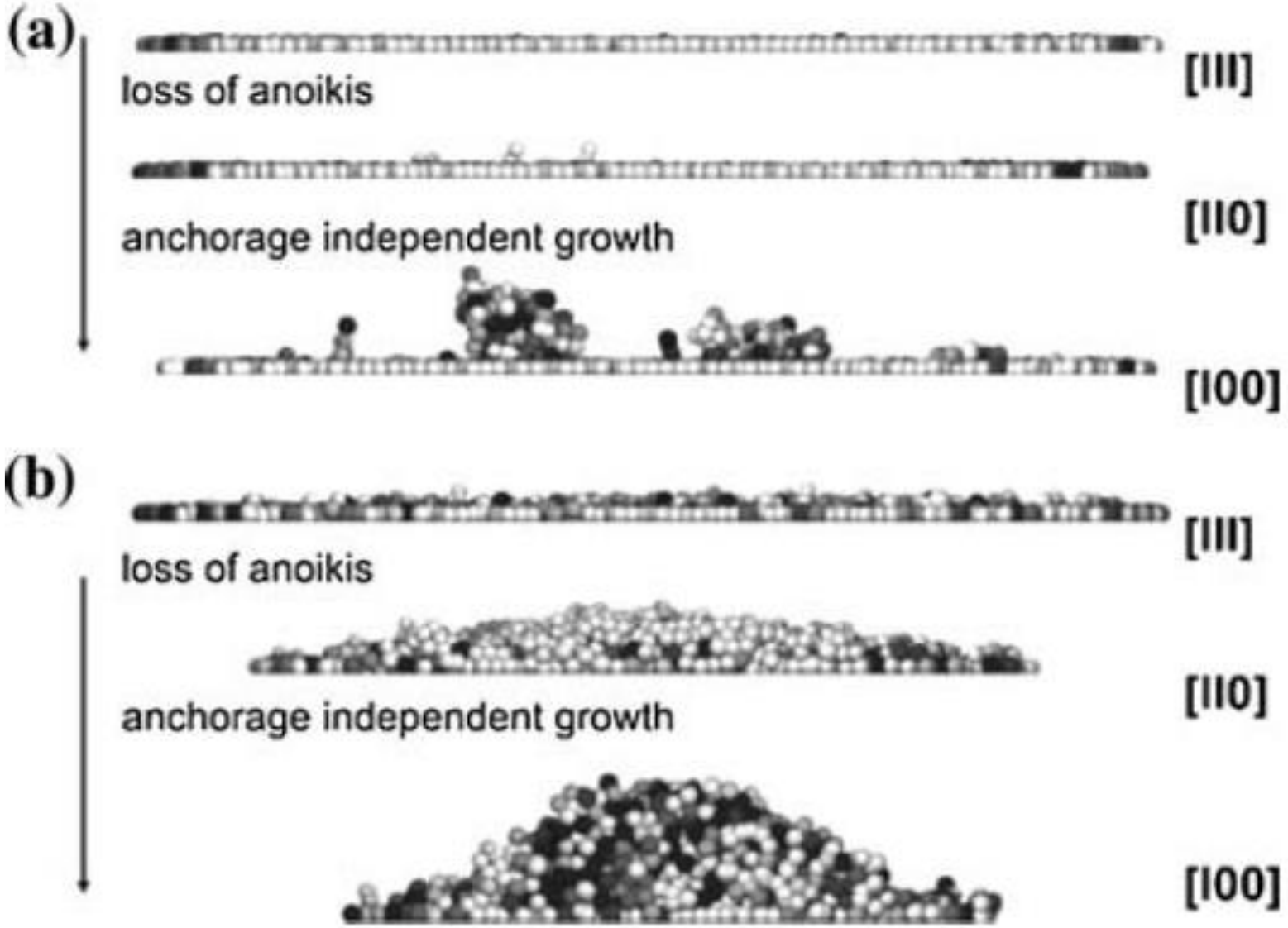

Fig. 5 Simulation of the growth of epithelial cell populations in vitro for cell substrate anchorage of (a) 600 lN/m and (b) 200 lN/m. [III]: contact inhibition, anchorage-dependent growth, and anoikis present. [II0]: contact inhibition and anchorage-dependent. [I00]: contact inhibition. (From Galle et al. , 2005)

Simulation of Bone Healing , Considering Growth of Fibrous Tissue and Cartilage

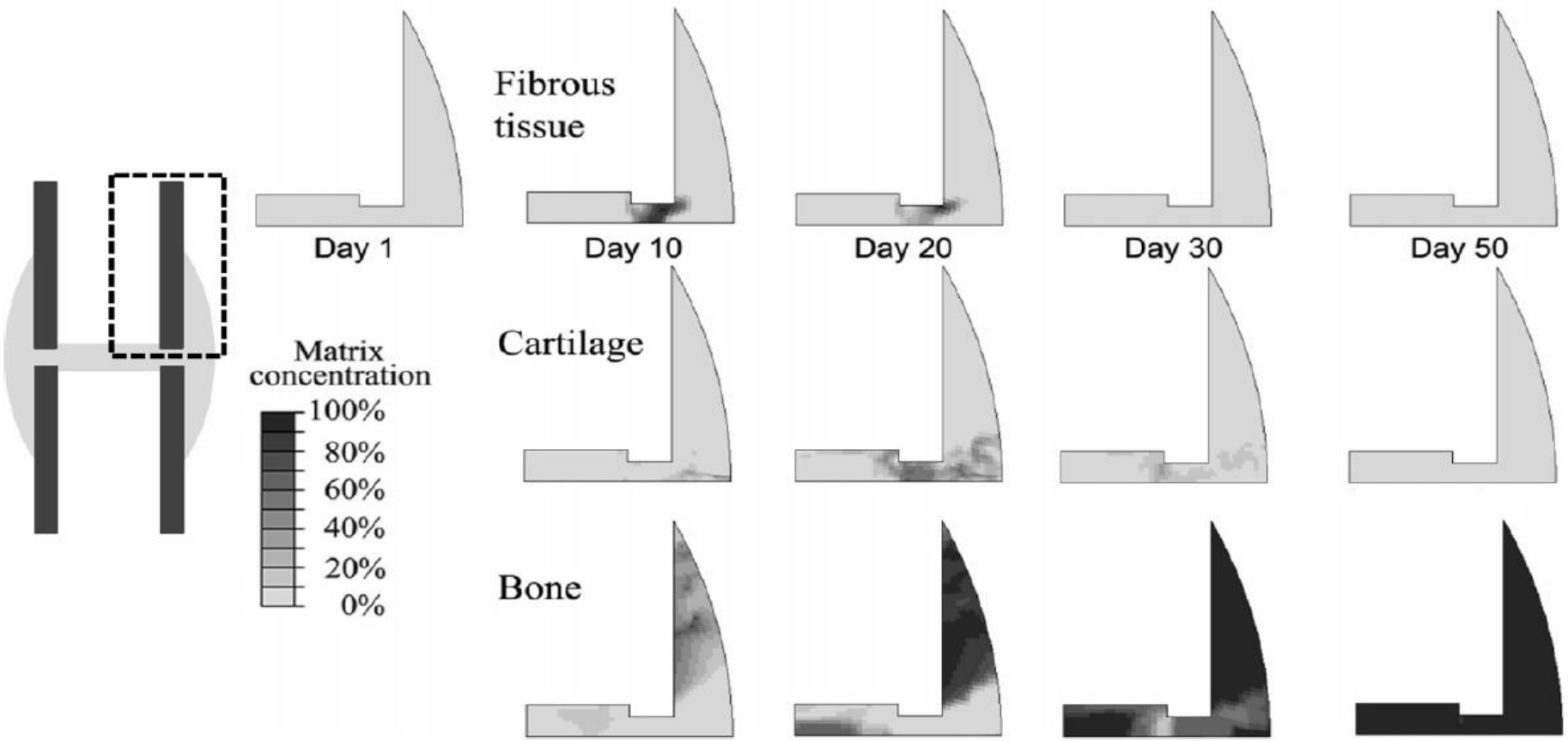

Fig. 10 (From Isaksson, 2008)

Simulation of Bone Healing. Finite Element Method Application

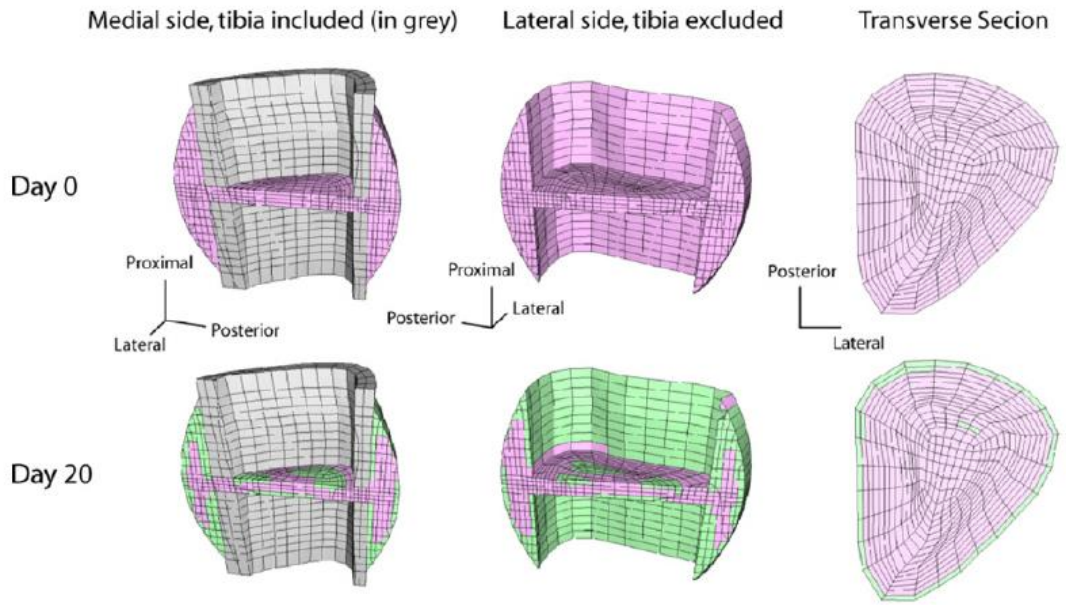

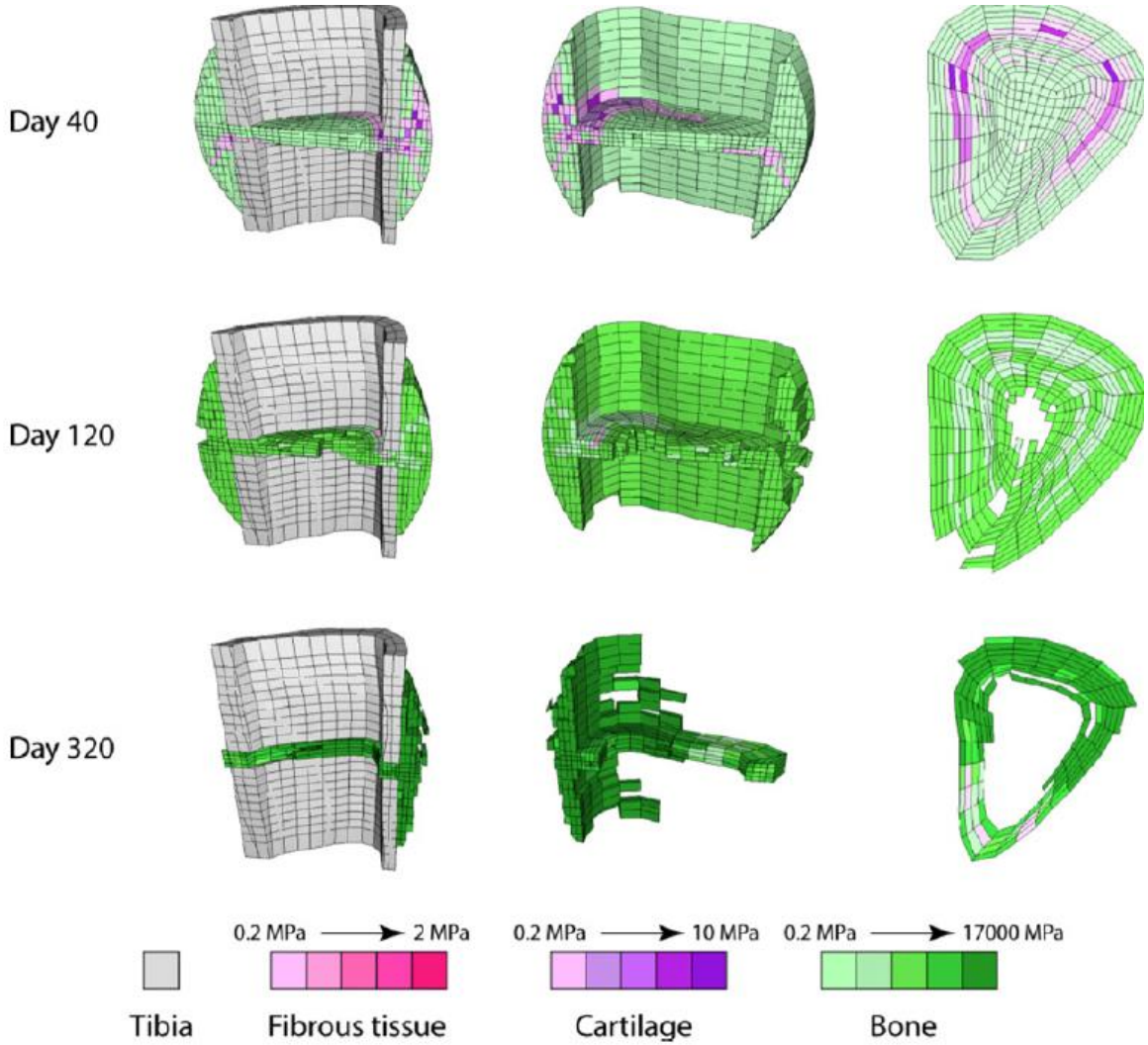

Fig. 11 (From Byrne et al., 2011)

Multi-Stage ASC Myogenesis. Reduction to a System of Nonlinear ODEs

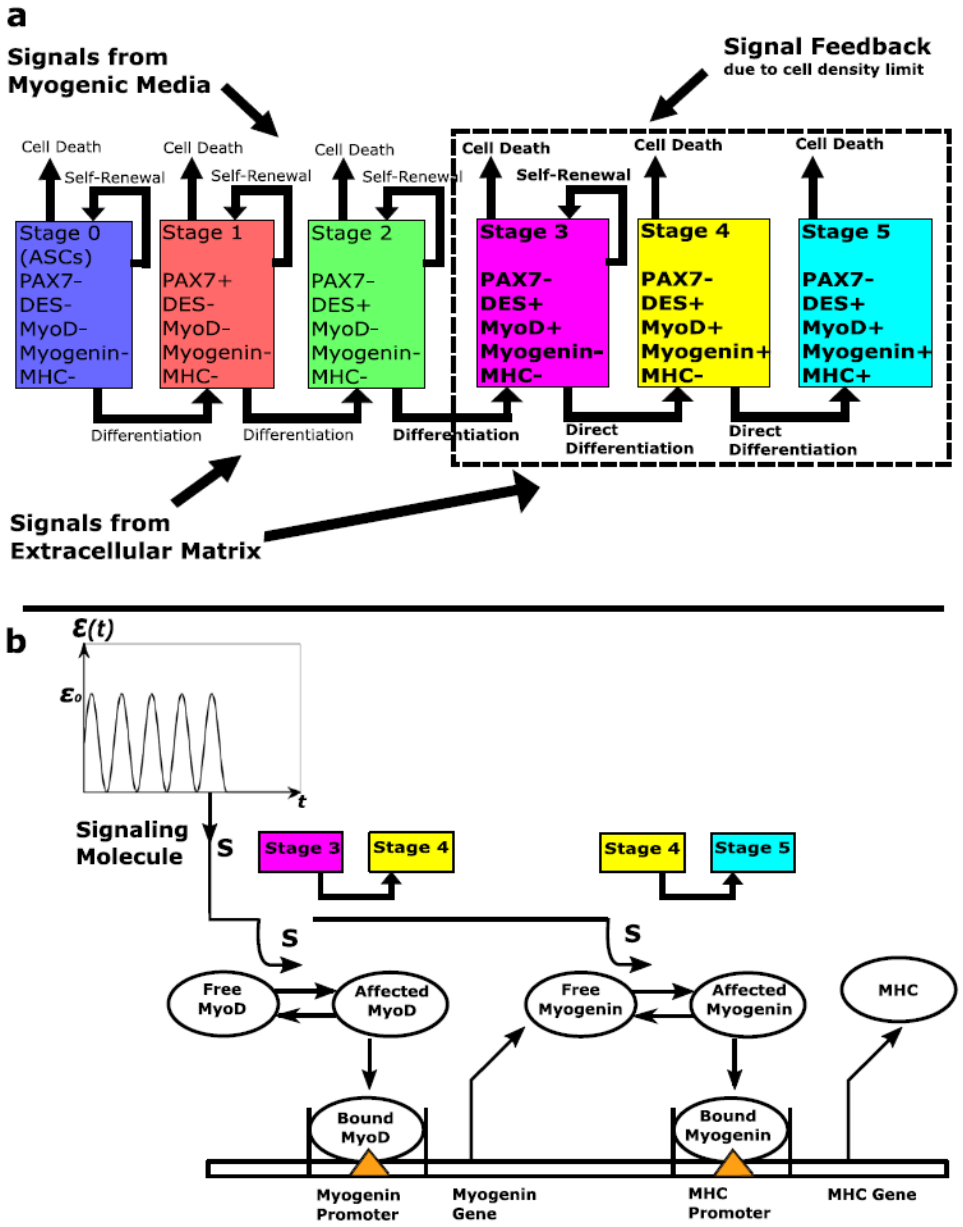

Fig. 12 (From Deshpande and Spector, 2017)

Kinetics of Cell Groups during ASC Myogenesis

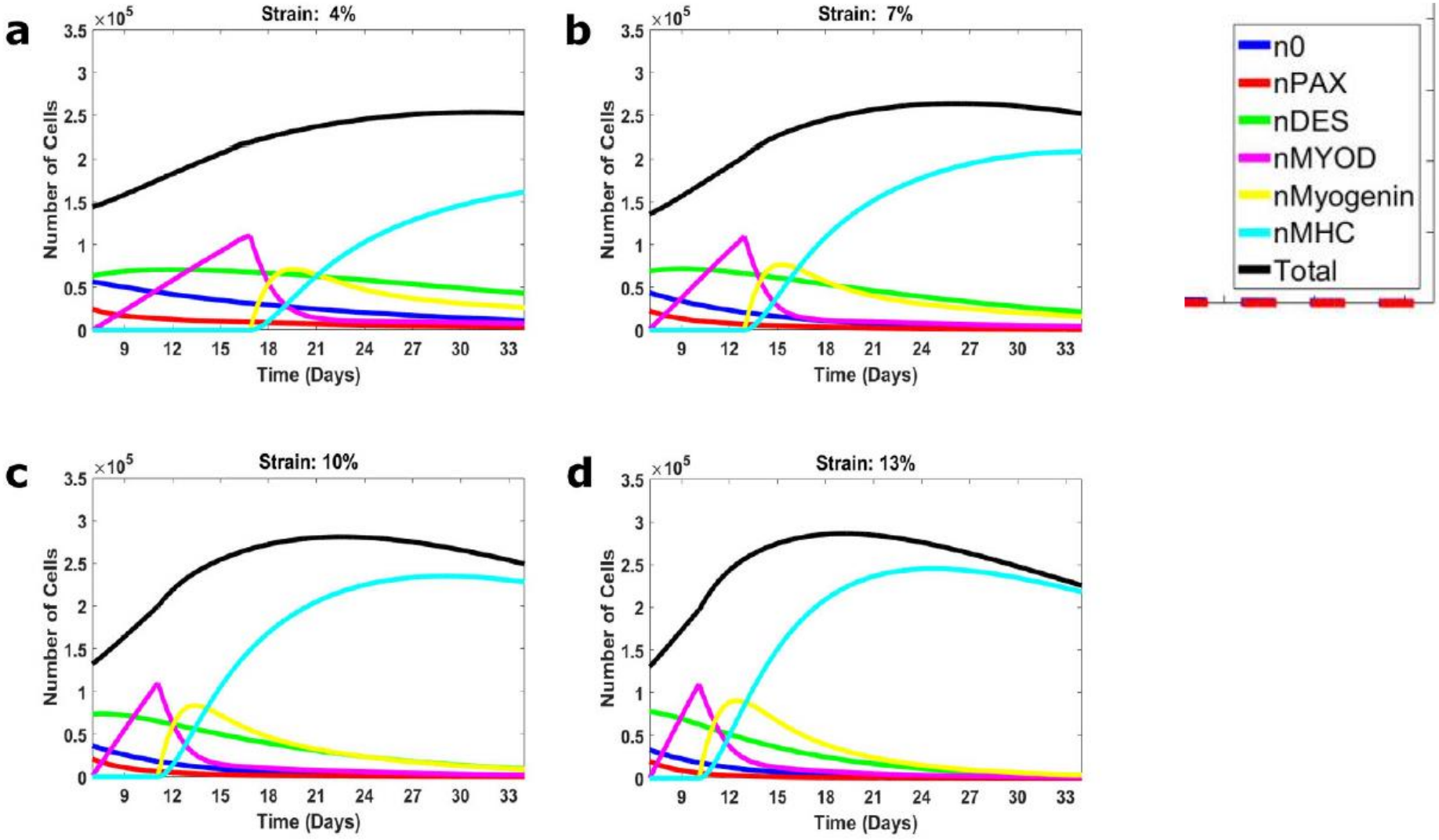

Fig. 13 (From Deshpande and Spector, 2017)